A comparison of bio-hydrodynamic interaction within mangrove and saltmarsh boundaries

Journal:	*Earth Surface Processes and Landforms*
Manuscript ID	ESP-15-0118.R2
Wiley - Manuscript type:	Paper
Date Submitted by the Author:	18-Apr-2016
Complete List of Authors:	Chen, Yining; Second Institute of Oceanography, SOA, Research Centre for Island Management and Exploitation; Xiamen University, State Key Laboratory of Marine and Environmental Science Li, Yan; Second Institute of Oceanography, SOA, Research Centre for Island Management and Exploitation; Xiamen University, State Key Laboratory of Marine and Environmental Science Cai, Tinglu; Second Institute of Oceanography, SOA,, Research Centre for Island Management and Exploitation Thompson, Charlotte; National Oceanography Center, School of Ocean and Earth Science Li, Yi; Second Institute of Oceanography, SOA,, Research Centre for Island Management and Exploitation
Keywords:	Mangrove, Saltmarsh, Hydrodynamics, Vegetation Drag

A comparison of biohydrodynamic interaction within mangrove and saltmarsh boundaries

Yining Chen[1,2]*, Yan Li[1,2], Tinglu Cai [1],Charlotte Thompson[3],Yi Li[1]

1. Second Institute of Oceanography, SOA, Hangzhou, 310012, China
2. State Key Laboratory of Marine and Environmental Science, Xiamen University, Xiamen, 361005, China
3. School of Ocean and Earth Science, National Oceanography Centre, Southampton, SO14 3ZH, UK

Abstract:

Mangrove forests and saltmarshes are recognized for their roles in wave and current attenuation, although a comparison of *in situ* observations between woody and herbaceous plants is needed in order to understand the different mechanisms of bio-physical interaction within coastal wetlands. The aim of our study was to compare the mechanisms of flow reduction and energy dissipation by mangrove trees and saltmarsh grass in a subtropical area where tidal currents dominate. Fieldwork was conducted to measure the hydrodynamic processes occurring at the boundaries between a bare mudflat and vegetated tidal flat, as the flow transitions from a bare mudflat to either mangrove or saltmarsh. Synchronous ADV measurements at three sites revealed that the mangrove was more effective than the saltmarsh grass at flow reduction. In addition, a considerable rotation in flow direction was observed as the flow entered the mangrove trees, while rotation was considerably less pronounced within the saltmarsh edge. The mechanism for

this difference was explained through a combination of changes in drag force and eddy viscosity over the two vegetation types. Although overall the mangrove was observed to dissipate energy more effectively than the saltmarsh, the relative efficiency of the vegetation at dissipating turbulent energy was found to vary with the maximum water level of tidal cycle. When the maximum water level remained below the mangrove canopy bottom ('bio-line'), the energy dissipation ability of the mangrove was relatively low, a result of the presence of rigid, sparse trunks rather than denser saltmarsh grass found near the bed; when the maximum water level was sufficiently high to reach the mangrove canopy, the ability of the mangrove to dissipate energy was significantly increased, becoming more effective than the saltmarsh grass.

Keywords: Mangrove; Saltmarsh; Hydrodynamics; Vegetation Drag

Introduction

Natural coastal wetlands are now widely recognized as potential buffers to waves and tidal flows, in addition to their global importance in ecosystem services (Perillo *et al*., 2009; Barbier *et al*., 2011; Moller, 2012; Moller *et al*., 2014). Saltmarsh and mangrove are common coastal wetland types globally, although the latter is restricted to tropical and subtropical regions. Generally, saltmarsh is characterized by herbaceous vegetation and mangrove by halophytic trees and shrubs (Mitsch and Gosselink, 2007). Both types of habitats can be used as tools for coastal defence, by taking advantage of their ability to reduce flow velocity, and to dissipate tidal and wave energy (Redfield, 1972; Gedan, 2001). Numerous studies have shown that saltmarsh grass canopies (e.g., *Spartina* canopy) can significantly modify the velocity profile of the water column to result in a reduction of the mean velocity (Shi, 1995; Fonseca, 1996; Bouma *et al.*, 2005; Neumeier, 2007). In some early work by Leonard and Luther (1995) using hot-film anemometry, a mean flow speed reduction from 9.2 cm s^{-1} in open water, to 5.2 cm s^{-1} in a sparsely vegetated area, and further to 2.8 cm s^{-1} in a densly vegetated area was observed in a *Spartina alterniflora* saltmarsh near Cedar Creek, Florida. Neumeier and Ciavola (2004) described their observations of vertical velocity profiles in a saltmarsh canopy using ADVs. At 15cm above the bed, the flow speed was reduced from a maximum of 10 cm s^{-1} over the bare mudflat to a magnitude less than 2.5 cm s^{-1} over an approximately 20 m wide area of *Spartina anglica* saltmarsh. Besides those fine scale studies, observations at larger scales have also revealed a decrease in flow velocity of up to one order of magnitude between saltmarsh and mudflat (Bouma *et al.*, 2005).

Meanwhile, mangrove trees have also been shown to alter flows due to the presence of trunks and aerial roots (Wolanski *et al.*, 1992; Furukawa *et al.*, 1997; Fischenich, 2000; Mazda *et al.*, 2005; Mazda, 2009). Available field measurements of flow variation through a main channel and into the mangrove interior have been reported by Mazda *et al*. (2004) and Kobashi and Mazda (2005), illustrating a reduction of flow speed from 10 cm s^{-1} to only 3-4 cm s^{-1} just 15 m from the mangrove edge, which was associated with a gradual change in flow direction.

The attenuation of turbulent energy by vegetation is an important process which has a significant influence on sediment transport, particle settling rates and the subsequent sedimentation processes and rates (Thompson *et al*., 2004; Neumeier and Amos, 2006; Neumeier, 2007; Zong and Nepf, 2010; Nepf, 2012; Ortiz *et al*., 2013; Moller *et al*., 2014). Compared with studies focused on the reduction of flow speed caused by vegetation, only limited field observations have been conducted to study turbulent energy attenuation within vegetated tidal flats. For example, Leonard and Luther (1995) reported that turbulence intensities on saltmarsh surface were as much as one order of magnitude less than turbulence intensities determined for adjacent tidal creek flows. Christiansen *et al*. (2000) observed a reduction of Turbulent Kinetic Energy (TKE) by at least a factor of 5 associated with saltmarsh vegetation adjacent to a creek bank. Further, because the aboveground biomass of saltmarsh grass generally decreases with height, the denser part of the grass canopy near the bed was more effective than the upper part at dissipating turbulence, giving an additional 20-35% reduction (Luther and Leonard, 1995; Neumeier and Amos, 2006). Due to the unique biophysiological characteristics of mangroves, such as their network of trunks and the aerial roots, the energy dissipation caused by mangrove is very complicated, and associated with the generation of eddies and wakes (Mazda *et al*., 1997; Massel *et al*., 1999; Mazda, 2009). However, few field observations have focused on the turbulence associated with biological properties, such mangrove roots, within the interior of mangrove forests (Wolanski *et al*., 1992; Furukawa *et al*., 1997). .

The mechanisms controlling flow velocity reduction and turbulence dissipation by plants have been studied by a number of researchers. In general, both mangrove trees and saltmarsh grass are responsible for enhancing bottom friction, as the vegetation presents an obstacle to the flow (Furukawa *et al*., 1997; Mazda *et al*., 1997; Nepf, 1999; Nepf, 2012), and the additional drag exerted by the plants reduces the mean flow (Nepf, 1999). Meanwhile, the vegetation converts mean kinetic energy to turbulent kinetic energy within stem wakes, to increase turbulence intensity: because this wake turbulence is generated at the stem scale, the dominant turbulent length scale is shifted downward dissipating any turbulent energy with greater length scales (Nepf *et al*., 1997; Nepf, 1999 and 2012). Consequently, the efficiency of either flow reduction or turbulence dissipation depends on specific vegetation properties. For saltmarsh grasses, the height, population density, stiffness and geometry of stems and blades determine these effects (Luther and Leonard, 1995;

Neumeier and Ciavola, 2004; Neumeier and Amos, 2006; Luhar *et al*., 2008; Nepf, 2012; Ortiz *et al*., 2013). Meanwhile, mangrove has dense canopies, together with rigid trunks and an aerial root network (Furukawa *et al*., 1997; Mazda *et al*., 1997). The dense network of trunks, branches and above ground roots of the mangrove causes much higher drag forces, and flows around individual trunks and roots generate eddies and wakes at their own scales (Furukawa *et al*., 1997; Quartel *et al.*, 2007). Therefore, the ability of the mangrove to retard flow and dissipate turbulence depends on the density of the forest, the diameter of the roots and trunks and the submerged portion of canopy (Massel *et al*., 1999; Mazda *et al*., 2005).

Understanding the ability of plants to protect shorelines allows us to evaluate the cost of wetland change or degradation and the value of restoration (Gedan *et al*., 2011). Coexistence of mangrove forests and saltmarshes occurs on many tidal flats and this causes spatial competition. For example, in Australia, a decline of saltmarsh was found as a result of the landward encroachment of mangroves (Saintilan and Williams, 1999). The encroachment rate of the mangrove was related to changes in sedimentation rates driven by biohydrodynamic interaction (Rogers *et al.*, 2006). On the contrary, in the southeast coast of China, the rapid spread of the saltmarsh grass *Spartina alterniflora* has been reported to affect the local mangroves (Lin, 2001; Zhang *et al*., 2012). Studies of the population dynamics and competition between local mangrove and the exotic saltmarsh grass in this region have been carried out (Zhang *et al*., 2012), but any link between the sediment dynamic process and the expansion of the *Spartina* saltmarsh in this region has not yet been examined. Therefore, there are strong grounds for a comparison of the bio-hydrodynamic interaction of saltmarsh and mangrove forests against the same physical background on the southeast coast of China.

In this paper, we aim to investigate and compare the influences of mangrove trees and saltmarsh grass on tidal flat hydrodynamics. In particular, we attempt to relate the mechanisms of flow mediation and energy dissipation by the two types of vegetation to their biological characteristics. To achieve this goal, synchronous measurements of hydrodynamic data were taken from three adjacent locations dominated by tidal currents: a bare mudflat, a mangrove edge and a saltmarsh edge.

Study Site

Yunxiao Mangrove National Natural Reserve, located within the turbidity maximum zone of the Zhangjiang Estuary in the southeast China coast, was selected for the field measurements (Figure 1). The runoff of the Zhangjiang River carries a large amount of fresh water and sediment, with an annually-averaged water discharge of $9.6\text{x}10^{8}$ m^3 and annually-averaged suspended sediment concentration of 380 mg L^{-1}. This suspended sediment concentration decreases to ~40mg L^{-1} within the estuary and further to ~ 30 mg L^{-1} in Dongshan Bay (MICZTWR Office, 1990; Liu, 1991). The annual precipitation in this region is 700 mm, 80% of which occurs in the wet season (April to September). Being a mesotidal (mean tidal range = 2.3 m) estuary, the Zhangjiang Estuary is dominated by irregular semi-diurnal tides and due to the sheltered conditions in Dongshan Bay, the wave conditions are insignificant outside of the typhoon seasons (Zheng *et al.*, 2009). The resulting physical conditions in the estuary favor the deposition of fine-grained sediments, which form a wide range of tidal flats along the main channel. The site under investigation is located at the apex of a channel meander, where a relatively wide tidal flat develops with a slope of 2-3‰. The bed of this tidal flat is mainly comprised of fine-grained clay and silt sediment with a medium grain size of 6-7 μm.

The upper part of the flat is occupied by native mangrove species (*K.obovata*, *A. corniculatum*, and *A. marina*), while the exotic *Spartina alterniflora* occupies part of the mudflat in front of the mangrove forest (Zhang *et al*., 2012). The mangrove trees at the front edge are normally shorter than those in the interior of the forest, because of the difference in age. The high density *Spartina alterniflora* formation usually reaches a maximum height of 1.5-2.0 m in autumn, and is restricted to the upper part of the mudflat. The grass in the lower part of the tidal flat was mowed regularly, due to intentional conservation efforts by the local management office to maintain a bare mud flat here (Zhang *et al*., 2006). The site is well managed for mangrove habitat protection purposes, and human activities are restricted to the lower part of the tidal flat.

A topographic map of the region is included in Figure 1, indicating a small elevation change (<0.27%) in the NW-SE direction, consistent with the tidal current axis. The elevation change between the measurement positions themselves is 0.05 m. A small tidal creek system has developed within the study area, which follows the main slope direction until it bifurcates. This feature has very low relief: the main creek channel is less than 5 cm in depth; the second order creek is only 1-2 cm in depth. Thus, this tidal creek system has minimal influence on the hydrodynamics.

Method

Field observations were carried out in Spring to coincide with the wet season and the start of the annual growing season. Measurements were undertaken over a period from spring to middle tides to ensure water depths were sufficient to cover the instrumentation.

Three locations (Figure 1) were selected for synchronous measurements: the bare mudflat (Location A), close to the edge of the vegetated areas; the mangrove edge (Location B); and the edge of a closed saltmarsh meadow

(Location C). A wooden pier (Figure 1d) provided access for the deployment. The pier was a raised platform that sits above the extreme high water level of this region and as such it had minimal influence on flows. In addition, the measurement locations were restricted to one side of this pier. The distance between each location was approximately 35 m, with vegetation extending approximately 10 m in the direction of the flood. Due to the limitations of instrument availability, only three ADVs were used in this study, based on the assumption that the flow over the bare mudflat was uniform throughout the proximal mudflat area. As such, both the mangrove and saltmarsh locations shared the same control point. Given the very small elevation changes over this area, this is a reasonable assumption.

Three velocity components, X, Y, Z, corresponding to eastward, northward and upward directions, were measured using a 3-D Acoustic Doppler Velocimeter (ADV; Nortek Vector). The ADV sensors were vertically positioned at 20 cm above the bed, with their measurement volumes 8 cm above the bed. The instruments were programmed to collect data continuously at 16 Hz. A compass was used to calibrate the direction of ADV sensors. Since ADV sensors are sensitive to obstacles, Location B was carefully chosen to avoid mangrove trunks, and a small plot beneath the ADV was cleared at Location C to minimize any direct influence of grass on the probe. A time series of velocity data was collected and the flow components were rotated horizontally to give

U, V, W, where U is the main flow in the flood direction on the bare mudflat, V is perpendicular to the main flow, and W is the upward component. The dataset was divided into 5-minute intervals for further data processing, assuming stationarity over this period. The phase-space thresholding method developed by Goring and Nikora (2002) was adopted for despiking noise before the calculation of mean and instantaneous velocities. The TKE density was estimated using:

$$TKE_{density} = \rho(\overline{U'^2} + \overline{V'^2} + \overline{W'^2}) \quad (1)$$

Where, ρ is the fluid density; U', V' and W' are the instantaneous velocities of three flow components

With regard to the relatively high position of the ADV pressure sensor, and the low submergence duration, it was not feasible to collect water level data using the ADV itself. An Optical Backscatter Sensor (OBS; manufactured by Campbell Scientific) with included pressure sensor was set up 20 cm above the bed at Location A, to collect a longer series of water level data at a rate of one sample per 20 seconds. The data were processed to obtain averaged values at the same time interval as the ADV data (5 minutes).

In addition, an RTK-GPS (Trimble-SPS881, ±1 cm in vertical accuracy) survey was undertaken to obtain bed form information and record the relative elevations of the three ADV deployments for water level analysis. The RTK

GPS survey showed that the bed elevations of Locations B and C were similar, 0.05 m higher than Location A. All of the water level data used in this study refer to the elevation above the mudflat bed at Location A. The biological properties of the vegetation, including trunk diameter, canopy properties and vegetation density, were measured *in situ*. A 25 cm×25 cm quadrate was used to sample *Spartina alterniflora* stands and aboveground biomass were measured by drying 5 plant samples collected randomly within the saltmarsh, cut into 10 cm vertical sections.

Results:

1) Vegetation measurements

The front edge of the mangrove forest was made up of a mixture of *K. obovata* and *A. corniculatum*, with a mostly (80-90 %) closed canopy. The mangrove trees were found to be young and short, having colonized this spot for only a few years. As such, a well developed aerial root system was not observed at the front edge, and the influence of roots could be neglected in this case. The trees had a mean height of 1.6m and the mean distance from the canopy to the bed was 40 cm (Table 1), resulting in a partial emergence of the canopy during the measurement period (Figure 2a).

Monotypic stands of dense *Spartina alterniflora* occurred at the seaward edge of the mangrove, extending to widths of tens - to - one hundred meters (Figure

1b). Only sparse patches of *Spartina alterniflora* could be found in the lower part of the flat. The *Spartina alterniflora* at Location C showed a high shoot density of 580 m^{-2} and high aboveground biomass of 2.5 kg m^{-2}, even early in the growing season (Table 1). More than 85% of the dry biomass was concentrated on the bottom 40cm and consequently the upper part of the canopy was less dense and more flexible. The canopy of the *Spartina alterniflora* reached a mean height of 1.0 m during this season, and was never fully submerged over the measurement period.

2) Water levels

The water level data throughout a spring to middle tidal cycle is shown in Figure 2a, including the records of 9 tidal cycles. The relationship between the water levels and vegetation characteristics is displayed in Figures 2b and 2c.

The mean water level was 0.43 m above the bed and the maximum water level reached 0.76 m (Figure 2). The diurnal inequality is notable in this area; on average, the maximum water level of nighttime tides was 0.3 m higher than the daytime tides, resulting in 80% longer periods of submergence.

The maximum water level of daytime tides was 45 cm above the mudflat bed (40 cm above the bed of the vegetated sites).This elevation is crucial for the vegetation, as it coincides with the bottom of mangrove canopy and contains nearly 90% of the dry biomass of the saltmarsh grass. This elevation can be regarded as the separation of the bio-hydrodynamic interaction, because it decides the influence of mangrove canopy on the hydrodynamic processes and the upper extent of the saltmarsh grass influence. For ease, the elevation of 45 cm above the mudflat bed was therefore defined as the 'bio-line' in the following text and graphs.

3) Flow variation through a spring to middle tidal cycle

Generally, the studied tidal flat was a low energy environment in the Spring, with a maximum flow speed of less than 0.22 m s^{-1} throughout the spring to middle tidal cycle (Figure 3). Although the vertical flow component is fundamental in terms of settling/resuspension processes, and a component of the TKE measurements, this section will focuses on the horizontal flow variation to demonstrate the bio-hydrodynamic processes.

Tidal currents at Location A (mudflat) flooded on a bearing of 305° and drained on a bearing of 124°. The mean resultant horizontal flow speed was 0.1 m s^{-1} (Figure 3, Table 2).

Both vegetation types significantly influenced the tidal currents in this area, although a difference existed in both the magnitude and controlling mechanisms between mangrove and saltmarsh plants. Comparing the flow speed data for all three locations, 50% and 40% reductions in mean flow speeds were found for the mangrove and saltmarsh edges respectively, 10 m from the vegetation boundaries in the flood direction.

For individual flow components, the reduction of the V component was less in the mangrove than in the saltmarsh edge, whilst the reduction in U component (main flood direction) was greater than in the mangrove edge than the saltmarsh edge (Table 2). The overall flow change caused by mangrove trees indicated that the trees rotated the flow into a direction perpendicular to the mangrove edge.

In fact, a substantial alteration in flow direction was observed within the mangrove trees, during both the flood and ebb stages. A flow deviation of 48° from the original direction was observed during floods and 30° during ebbs (Figure 3, Table 2).The mediation in flow direction by saltmarsh vegetation on the other hand appears limited (Figure 3 and Table 2), only deviating 15° at flood stage and 4° at ebb stage.

4) Energy dissipation through a spring to middle tidal cycle

Figure 4 and the energy data displayed in Table 2 show the turbulent energy dissipation at the mangrove and saltmarsh edges. Both mangrove trees and saltmarsh grass had notable influences on turbulence dissipation. The mean

TKE density dropped 92% in the mangrove edge and 86% in the saltmarsh edge, thus, the mangrove edge was relatively better at dampening high frequency energy over a spring to middle tidal cycle.

The TKE density showed a remarkable tidal asymmetry over the bare mudflat site, being much greater during the flood than the ebb. This was due to the turbulence of the currents being dissipated over the upper part of tidal flat during the flood stage, driven by the presence of vegetation. By contrast, this asymmetry was almost reversed at the vegetated sites. For most of the tidal cycles, the TKE density from both the mangrove and saltmarsh sites showed no clear dominance. The reason accounting for this change in tidal asymmetry might be that most of the energy was dampened at the front edges of vegetation and the vegetation in the upper part of the tidal flat only minimally absorbed turbulent energy, as such, the tidal asymmetry tended to be no clear dominance; secondly, during the ebb stage, as the flow passed the vegetation area to the bare mudflat, additional shear was created as a result of the change from a 'layered' to a single depth system.

Discussions

1) Mechanisms associated with flow reduction

The reduction of flow velocity within the vegetated mudflat is a function of drag forces and/or changes to the eddy viscosity, as described by previous models

(Mazda *et al*., 1997; Furukawa *et al*., 1997; Nepf, 1999; Koshiba and Mazda, 2005). Although field measurements of flow changes within mangrove forests are very limited, both our results and previously published data imply a rotation of the flow into the direction normal to the mangrove edge. To explain this rotation, an attempt is made here to assess possible mechanisms using two established models, one designed for the interior of a vegetated flat and the other for the front edge (Mazda *et al*., 1997; Koshiba and Mazda, 2005). The first model describes the drag force within a mangrove swamp interior close to a tidal creek, based on a momentum balance analysis for each fluid mass unit (Mazda *et al*., 1997, Equation 2, Figure 5a). In this model, the flow in the swamp interior is normal to the creek edge (also the vegetation edge) and the drag force ($F_{drag,x}$) caused by the vegetation is the main mechanism for flow reduction.

$$\frac{\partial u}{\partial t} + u\frac{\partial u}{\partial x} = -g\frac{\partial \varsigma}{\partial x} + F_{drag,x} \qquad (2)$$

where, u is the flow component normal to the vegetation edge, t is time, x is the distance into the swamp, g is acceleration due to gravity, ς is water surface elevation. The drag force can be expressed in a form relevant to the biological properties of the vegetation as:

$$F_{drag,x} = \frac{1}{2}C_D A u^2 \qquad (3)$$

where C_D is the drag coefficient and A is the total projected area of the vegetation (obstacles) per unit volume. This model provides a quantitative method of solving the drag coefficient when only the drag force is considered in terms of the impact of the vegetation.

The second model (Koshiba and Mazda, 2005, Figure 5a) deals with flow reduction in an area proximal to a creek, where the flow runs predominantly parallel to the channel. In this model, flow reduction is a function of both the drag force and an eddy viscosity term, as described below:

$$\frac{\partial v}{\partial t}+v\frac{\partial v}{\partial y}+u\frac{\partial v}{\partial x}=-g\frac{\partial \varsigma}{\partial y}-\frac{C_D}{Le}v|v|+f\frac{\partial^2 v}{\partial x^2} \quad (4)$$

where, v is the flow component parallel to the vegetation edge, y is the distance parallel to the edge, Le is the effective length scale of the vegetation, and f is the coefficient of the dynamic eddy viscosity. The second term in the right side of Equation 5 represents the lateral drag force created by the vegetation and the third term is the eddy viscosity, a function of turbulent stresses within the flow.

In order to use the models, the measured flow components U and V were rotated to obtain the components normal (u) and parallel (v) to the vegetation edge (see Figure 1b for this rotation). The flow rotation observed in our study is best explained through a combination of both models. The flow reduction in the direction normal to the vegetated edge (u) was similar to the scenario described in the first model (Mazda *et al*., 1997), a result of the drag force generated by the vegetation, while the flow reduction parallel to the edge was a function of both the drag force and changes to the eddy viscosity term as described in the second model (Koshiba and Mazda, 2005), a result of increased momentum fluxes within the flow.

To confirm these results, we undertook a further analysis of the two models to link them to the bio-hydrodynamic processes. The relationships between u and v components from all three sites are displayed in Figure 6. As the tidal currents flowed from the mudflat to the mangrove and saltmarsh edges, significant linear relationships could be found between the u components, with high R-squared values (>0.9). However, for the v component, a linear relationship occurred between the mudflat and the saltmarsh edge (R-squared>0.9). A reduction of the v component occurred between the bare mudflat and the mangrove edge, representing a near total reduction in velocity (mean v decreases from 0.07 m s^{-1} to 0.01 m s^{-1}). It appeared that the saltmarsh grass reduced tidal currents in a linear way both in u and v direction, but the mangrove trees resulted in a linear reduction in one direction (u), and a non-linear reduction in the other (v).

The reduction in the u component for both types of vegetation could easily be explained by the added drag force generated by the vegetation as described by Mazda *et al*. (1997), and indicated by the clear linear relationships between the flow components of vegetated locations and the bare mudflat (Figure 5b,c).

However, at the edge of mangrove forest, the v component exhibited a notable non-linear reduction in comparison to flow on the bare mudflat (Fig 6). The mechanism for this can be related to both the additional drag force, plus the alteration of the eddy viscosity term as shown by Kobarshi and Mazda (2005). The non-linear relationship between the v component of mangrove and mudflat, together with the strong velocity gradient between the mudflat and the mangrove in the direction of the v component, indicates that momentum fluxes due to local energy production and dissipation by turbulent eddies was more likely to be the primary mechanism accounting for the flow reduction parallel to the mangrove edge (Figure 5b).

In order to compare the overall properties of the vegetation, the drag coefficient imparted upon flows can be estimated. In this study, the tidal currents flowed across a low gradient flat, leading to a minimal water surface gradient between three sites. Thus, the first term in the right side of Equation 2 was eliminated. The first term in the left side was also neglected because of the long wavelength of the tides. Combining Equations 2 and 3, we obtained a formula to calculate the drag coefficient:

$$C_D = \frac{2}{Au}\frac{\partial u}{\partial x} \quad (5)$$

Thus, the drag coefficient C_D 8 cm above the vegetated bed was estimated and the term $C_D A$ used to describes the bulk drag coefficient for vegetation (Wang *et al.*, 2004).In the saltmarsh, A (total projected area of vegetation) was estimated using biomass data and 90% vegetation coverage, based on field observation. Below the mangrove canopy, the diameter (0.1 m) and spacing (0.7 m), together with the varying water level, was used to estimate A for the mangrove trunks. Within the mangrove canopy, 80% closure was used, along with the water level data, to estimate the total projected area of the vegetation.

The drag coefficient C_D over a smooth mudflat surface was calculated based on shear stress values estimated using the Reynold Stress and Quadratic Stress Laws, been found to be similar at low velocities (Thompson *et al*., 2003),using the equation below:

$$\tau_x = -\rho \overline{u'v'} = 0.5 \rho C_D u^2 \quad (6)$$

Where τ_x is the shear stress, u' and v' are the instantaneous velocities of the normal flow component and the parallel flow component, the u is the mean velocity normal to the edge at 8 cm above the bed and C_D is the ‘apparent drag coefficient’ at the measurement height (Wang *et al.*, 2004).

Estimates of C_D for the three locations are listed in Table 2; within the vegetation， it varied between 10^{-1} to 10^{0} as the water level changed, similar to other observations and simulations (Mazda *et al*., 1997; Fischenich, 2000; Li *et al*., 2012). The C_D estimated by this study showed a low mean value over the mudflat, a moderate value at the saltmarsh edge and a high value at the mangrove edge (Table 2), demonstrating the ability of the vegetation to enhance apparent bed roughness. The resistance to the flow presented by mangroves is therefore greater than that of the saltmarsh grass, consistent with the observed flow reduction in this direction (Table 2).

2) **Application of refraction theory for vegetation induced flow rotation**

Besides the models discussed above, another simple physical theory might be able to explain the phenomena observed by this study. The interaction of water waves with periodic structures, such as ripples and periodic cylinder arrays, can lead to refraction (Hu and Chan, 2005). For water waves much longer than the scale of obstacles, the analytic study by Hu and Chan (2005) found that a periodic cylinder array system mounted on the bottom behaved as an effective medium to generate refraction, based on photonic refraction theory. We adapt this concept to provide a simple explanation for the rotation of flows close to the vegetation boundary, to avoid the complexity of force and momentum balance analyses. Vegetated flat beds can cause refraction as the tidal waves propagating into them from the unvegetated tidal flat have very long wavelengths in relation to the scale of the vegetation; it should be noted however that the uneven distribution and structure of natural vegetation would add a further level of complexity. For simplicity, Snell's Law (Equation 7) can be applied to examine the refraction caused by both the mangrove trees and saltmarsh grass.

$$\frac{\sin\theta_1}{\sin\theta_2} = \frac{c_1}{c_2} = \frac{n_2}{n_1} \qquad (7)$$

Where θ_1 is the incident angle, θ_2 is the refractive angle, c_1 (= $\sqrt{gh}$ =2.2 m s^{-1} in this study) and c_2 are the phase velocities of tidal waves in the bare mudflat ($_1$) and in the vegetated flat ($_2$), and n_1 and n_2 are the refractive indices of the respective mediums (the refractive index of the mudflat n_1 =1).

The general trend of the vegetation boundary along the coast (170°) was taken as the interface for incidence and refraction, representing a change in medium. The estimate of c_2 was calculated using the known values of θ_1, θ_2 and c_1, which showed the tidal wave speed reduces from 2.2 m s^{-1} in the bare mudflat to 0.8 m s^{-1} in the mangrove edge and to 1.8 m s^{-1} in the saltmarsh edge. It appears that mangrove trees (refractive index=2.8) were more refractive than saltmarsh grass (refractive index=1.2). This refraction estimate, considers the vegetation edge as a change in medium, producing a single impact on the direction of the tidal wave, when, in reality, the phenomenon would be a function of multiple refraction events as the waves passes multiple rows of trunks, complicated by changes in trunk density and size. The results however, represent an averaged condition, and highlight the differences in the impact of woody and herbaceous vegetation types on the tidal wave. While further theoretical investigation is needed, this simple method may be useful for future coastal protection planning using vegetation, to predict the general flow rotation caused by different species.

3) Energy dissipation of two types of vegetation

For different vegetation species, the relative efficiency of the flow reduction by turbulent energy dissipation is important from the perspective of coastal engineering. As noted by previous researchers, the impact of vegetation on hydrodynamics is associated with changes in the water level relative to vegetation height, which determines the status of emergence or submergence. In the field, Mazda *et al*. (2006) pointed out that wave energy reduction by mangroves increased when the water level rose to the height of canopy. Laboratory studies have also indicated the importance of the spatial structure of vegetation in moderating the hydrodynamics (e.g., Luhar *et al*., 2008; Tanino and Nepf, 2008; Ortiz *et al*., 2013). Laboratory studies have revealed the differences in mean and turbulent flow, and mass transport between emergent canopy and submerged canopy (Nepf, 2012). Mangrove forest is made up of rigid trunks with large spacing at the lower part, which support dense and close leaves and stems on the top. Saltmarsh grass has dense stems and leaves concentrated at the lower part whilst the tips are more sparse and flexible than the lower part. Therefore, an attempt was made to examine the relationship between turbulent energy dissipation by vegetation dependent on the relative water level.

The maximum water level of each tidal cycle was plotted against the TKE density for the bare mudflat (Figure 7a). A significant linear relationship was observed indicating the dependency of TKE density on the water depth. TKE density dissipation percentage was defined as the percentage ratio of tidally-averaged TKE reduction by vegetation to the energy density of the mudflat, indicating the effectiveness of the vegetation at damping turbulent energy. Figure 7b illustrates the variations in energy dissipation with maximum water level of each tide for the mangrove and saltmarsh grass, showing a considerable difference between the vegetation types. When the maximum water level was low, and below the bio-line, the saltmarsh grass showed a higher TKE dissipation percentage than the mangrove; when the maximum water level increased above the bio-line, mangrove was more effective in dissipating the turbulent energy.

As previously mentioned, the bio-line marks the change from mangrove trunk to mangrove canopy, as well as the change in density of the saltmarsh grass. The mangrove displayed a linear increase in TKE dissipation percentage with maximum water level, indicating that the canopy with leaves and stems was better than the rigid trunks at suppressing turbulence. The integral length scale of the turbulence for rigid vegetation has been found in laboratory studies to be related to the stem diameter and spacing, regardless of the water depth (Tanino and Nepf, 2008). Thus, as the water level rose to the dense canopy, and a greater portion of the high-density canopy is submerged, the mangrove becomes more effective than the saltmarsh grass at dissipating turbulence.

Nepf (2012) summarized the bio-hydrodynamic interaction for both emergent and submerged canopies. Emergent canopies, as described by Nepf (2012), dissipate eddies with scales greater than the scales of the stem, determined by their spacing and diameter, while contributing additional turbulent energy at these stem scales. Thus, the dominant turbulent length scale within a canopy was shifted downward compared with the non-vegetated flat. When the maximum water level was below the bio-line, the saltmarsh grass showed a higher TKE dissipation percentage than the mangrove, due to the high density of grass stems and leaves.

Once the maximum water level reached 0.5 m, more than 90% of the saltmarsh grass biomass was submerged to form a submerged canopy. As described by Nepf (2012), the drag discontinuity at the top of the submerged canopy generated a shear layer, the impact of which persisted a certain distance to separate the canopy into two regions: energetic turbulent transport in the upper canopy and diminished turbulent transport in the lower part. The combination of these two layers determines the overall dissipation ability of the canopy as a whole, which showed an overall decrease in dissipation percentage, and scatter in the data with water level increased.

Although the mangrove was found to be more effective overall than saltmarsh grass at dissipating turbulent energy over a spring to middle tidal cycle (Table 2), their abilities varied with relative water level and the consequent status of emergence/submergence. For mangrove, their trunks showed less TKE dissipation than the grass, until the dense canopy of the mangrove contributes to the turbulent process, where their dissipative ability exceeds that of the grass. The ability of the saltmarsh grass itself to dissipate turbulence was also associated with emergence/submergence, but was generally more effective than mangrove only at low tides when it occupied a larger percentage of the water column. Therefore, for coastal protection purpose, herbaceous plants should be a better choice to protect coasts with small tidal ranges, whilst woody plants could be more effective for large tidal range coasts or coasts with significant waves.

Conclusions

In this contribution, we conducted a comparative investigation of the influence of mangrove and saltmarsh on tidal flat hydrodynamics, through synchronous field observations on a bare mudflat and within the boundaries of a mangrove and a saltmarsh. The results highlight the similarities and differences between woody and herbaceous plants in terms of their bio-hydrodynamic interactions, including:

1) Both mangrove trees and saltmarsh grass radically reduce flow speed, in comparison with a bare mudflat. Within the edge of a mangrove stand, the flow speed decreased by 50% in magnitude, greater than that observed in the margins of the saltmarsh. A considerable flow rotation was observed in the mangrove, whilst only a slight change occurred for flow direction in the saltmarsh.
2) The difference between flow alterations in the two vegetation types could be explained by the relative strength of the drag force and eddy viscosity caused by the vegetation. In addition, a simple method based on refraction theory was proposed to estimate the flow rotation differences between the trees and grass.
3) The mangrove was more effective at dissipating turbulent energy than the marsh, although both reduced the turbulent energy by over 86% compared to the bare mudflat. The relative turbulent energy dissipation efficiency of the two types of plants was related to the maximum water level of a tidal cycle. A 'bio-line' was defined to mark the elevation of vegetation influence. When the maximum water level was above this 'bio-line', the mangrove was more effective than the saltmarsh grass in dissipating turbulence and vice versa, due to the structural properties of the plants.
4) Regarding regional coastal protection, mangrove trees were found to be a better choice than saltmarsh grass in terms of stabilizing the coasts in this mesotidal estuary. The results indicated that a mangrove forest was likely

to reduce flow energy effectively at relatively low elevations where the water level is able to reach its canopy. Establishment of saltmarsh grass is more suitable for a higher elevation where the dense part of grass could effectively retard flow and turbulence. In addition, seasonality must be considered in future research when comparing the bio-hydrodynamic interaction of both mangrove and saltmarsh, because saltmarsh grass dies back in winter, whilst the mangrove persists year round.

Acknowledgement:

We would like to thank Prof. Yu Zhang and Dr. Yihui Zhang at Xiamen University for their valuable comments on this manuscript. Mr. Xinkai Wang and Mr. Yang Yang (SIO, SOA) are thanked for their support in fieldwork. Thanks extend to the Management Office of Yunxiao Mangrove National Nature Reserve, for the site access. Part of the instrumentation used in this study was provided by Prof. Yaping Wang at Nanjing University. This work is funded by NSFC Projects (Grant no. 41006047 and 40806038) and a Fundamental Research Fund of Second Institute of Oceanography (No.14252-80). The authors also thank the anonymous reviewers for their time and thoughtful comments.

References

Barbier EB, Hacker SD, Kennedy C, Koch EW, Stier AC, Silliman B. 2011. The value of estuarine and coastal ecosystem services.Ecological Monographs, 81(2), 169-193.doi: 10.1890/10-1510.1

Bouma TJ, Vries MBD, Low E, Kusters L, Herman PMJ, Tánczos IC, Temmerman S, Hesselink A, Meire P, Regenmortel SV. 2005. Flow hydrodynamics on a mudflat and in salt marsh vegetation: identifying general relationships for habitat characterisations. Hydrobiologia 540: 259-274. DOI: 10.1007/s10750-004-7149-0

Christiansen T, Wiberg PL, Milligan TG. 2000. Flow and Sediment Transport on a Tidal Salt Marsh Surface. Estuarine, Coastal and Shelf Science 50: 315-331. DOI: 10.1006/ecss.2000.0548

Fischenich C. 2000. Resistance due to vegetation. EMRRP Technical Notes Collection (TN-EMRRP_SR_07). U.S. Army Engineer Research and Development Centre, Vicksburg, MS. 9.

Fonseca, MS. 1996. The role of seagrass in nearshore sedimentary processes: a review. In: Nordstrom, K.F. and Roman, C.T.(eds.), Estuarine shores: evolution, environments and human alterations. Chichester, England: John Wiley and Sons, pp. 261–286.

Furukawa K, Wolanski E, Mueller H. 1997. Currents and sediment transport in mangrove forests. Estuarine Coastal and Shelf Science 44: 301-310. DOI: DOI 10.1006/ecss.1996.0120

Gedan KB, Kirwan ML, Wolanski E, Barbier EB, Silliman BR. 2011. The present and future role of coastal wetland vegetation in protecting shorelines: answering recent challenges to the paradigm. Climatic Change 106: 7-29. DOI: 10.1007/s10584-010-0003-7

Goring DG, Nikora VI. 2002. Despiking acoustic Doppler velocimeterdata. Journal of Hydraulic Engineering, ASCE 128: 117–126.DOI:10.1061/(ASCE)0733429(2002)128:1(117)

Hu X, Chan, CT. 2005. Refraction of Water Waves by Periodic Cylinder Arrays.Physical Review Letters, 95: 154501.doi: 10.1103/PhysRevLett.95.154501

Kobashi D, Mazda Y. 2005. Tidal Flow in Riverine-Type Mangroves. Wetlands Ecology and Management, 13: 615-619. DOI: 10.1007/s11273-004-3481-4

Leonard LA, Luther ME. 1995. Flow hydrodynamics in tidal marsh canopies.

Limnology and Oceanography, 40: 1474-1484

Li L, Wang XH, Williams D, Sidhu H, Song D. 2012. Numerical study of the effects of mangrove areas and tidal flats on tides: A case study of Darwin Harbour, Australia. Journal of Geophysical Research, 117. DOI: 10.1029/2011jc007494

Lin P. 2001. A review on the mangrove research in China. Journal of Xiamen University (Natural Science), 40: 592-603 (in Chinese)

Liu Q. 1991. Silt transportation and its influences on submarine scour and silting in Dongshan Bay, Fujian Journal of Oceanography in Taiwan Strait 10: 69-76 (in Chinese)

Luhar M, Rominger J, Nepf H. 2008. Interaction between flow, transport and vegetation spatial structure. Environmental Fluid Mechanism, 8.5-6: 423-439. doi:10.1007/s10652-008-9080-9.

Massel SR, Furukawa K, Brinkman RM. 1999.Surface wave propagation in mangrove forests. Fluid Dynamic Research, 24: 219–249.doi:10.1016/S0169-5983(98)00024-0

Mazda Y. 2009. Hydrodynamics and Modeling of Water Flow in Mangrove Areas. In Coastal Wetlands: An Integrated Ecosystem Approach, Gerardo M. E. Perillo EW, Donald R. Cahoon, Mark M. Brinson (ed). Elsevier; 231-262.

Mazda Y, Kobashi D, Okada S. 2005.Tidal-Scale Hydrodynamics within Mangrove Swamps. Wetlands Ecology and Management, 13: 647-655. DOI: 10.1007/s11273-005-0613-4

Mazda Y, Okada S, Kobashi D. 2004. Tidal flow mangrove forests and the eddy viscosity. Journal of the School of Mairne Science and Technology, 1: 29-35

Mazda Y, Wolanski E, King B, Sase A, Ohtsuka D, Magi M. 1997. Drag force due to vegetation in mangrove swamps. Mangroves and Salt Marshes, 1: 193-199

MICZTWR Office, 1990. Multipurpose Investigation of the Coastal Zone and Tidal Wetland Resources – Report of Fujian Province. Ocean Press, China.(in Chinese).575pp.

Mitsch WJ and Gosselink JG. 2007. Wetlands. Wiley. 619pp.

Moller I, Kudella M, Rupprecht F, Spencer T, Paul M, van Wesenbeeck BK, Wolters G, Jensen K, Bouma TJ, Miranda-Lange M, Schimmels S. 2014. Wave attenuation over coastal salt marshes under storm surge conditions. Nature Geoscience, 7: 727-731. DOI: 10.1038/ngeo2251

Moller I, Spencer T, French JR, Leggett DJ, Dixon M. 1999. Wave transformation over salt marshes: A field and numerical modelling study from north Norfolk, England. Estuarine Coastal and Shelf Science, 49: 411-426. DOI: DOI 10.1006/ecss.1999.0509

Moller I, 2012. Bio-physical linkages in coastal wetlands – implications for coastal protection. Jubilee Conference Proceedings, 51-60. DOI: 10.3990/2.170.

Nepf H, Sullivan J, Zavistoski R. 1997. A model for diffusion within emergent vegetation. Limnology and Oceanography,42(8): 85-95.

Nepf H. 1999. Drag, turbulence, and diffusion in flow through emergent vegetation. Water Resources Research, 35: 479-489. DOI: 10.1029/1998wr900069

Nepf H. 2012. Flow and transport in regions with aquatic vegetation. Annual

Review of Fluid Mechanism, 44:123-42. doi: 10.1146/annurev-fluid-120710-101048.

Neumeier U. 2007.Velocity and turbulence variations at the edge of saltmarshes. Continental Shelf Research 27: 1046-1059. DOI: 10.1016/j.csr.2005.07.009

Neumeier U, Amos CL. 2006. Turbulence reduction by the canopy of coastal Spartinasalt-marshes. Journal of Coastal Research, SI39: 433-439

Neumeier U, Ciavola P. 2004. Flow Resistance and Associated Sedimentary Processes in a SpartinamaritimeSalt-Marsh. Journal of Coastal Research, 20: 435-447. DOI: 10.2112/1551-5036(2004)020[0435:FRAASP]2.0.CO;2

Ortiz A, Ashton A, Nepf H. 2013. Mean and Turbulent Velocity Fields Near Rigid and Flexible Plants, and the Implications for Deposition. Journal Geophysical Research - Earth Surface, 118: 1-15. doi: 10.1002/2013JF002858.

Perillo GEM, Wolanski E, Cahoon DR, Brinson MM. 2009. Coastal Wetlands: An Integrated Ecosystem Approach. Elsevier: Elsevier B.V.

Quartel S, Kroon A, Augustinus PGEF, Van Santen P, Tri NH. 2007. Wave attenuation in coastal mangroves in the Red River Delta, Vietnam. Journal of Asian Earth Sciences, 29: 576-584. DOI: 10.1016/j.jseaes.2006.05.008

Tanino Y and Nepf H. 2008. Laboratory investigation on mean drag in a random array of Rigid, Emergent Cylinders. Journal of Hydraulic Engineering, 134(1): 4-41, doi: 10.1061/(ASCE)0733-9429(2008)134:1(34).

Redfield AC. 1972.Development of a New England salt marsh. Ecological Monographs, 42: 201–237

Rogers K, Wilton, KM, Saintilan N, 2006. Vegetation change and surface elevationdynamics in estuarine wetlands of southeast Australia. Estuarine, Coastal and Shelf Science, 66:559-569.

Saintilan N, Williams RJ. 1999. Mangrove Transgression into Saltmarsh Environments in South-East Australia. Global Ecology and Biogeography, 8: 117-124. DOI: 10.1046/j.1365-2699.1999.00133.x

Soulsby R. 1997. Dynamics of Marine Sands: A Manual for PracticalApplications. Thomas Telford: London.

Thompson CEL, Amos CL, Jones TER, Chaplin J. 2003. The manifestation of fluid-transmitted bed shear stress in a smooth annular flume-a comparison of methods.Journal of Coastal Research, 19(4), 1094-1103.

Thompson CEL, Amos CL, Umgiesser G. 2004. A comparison between fluid shear stress reduction by halophytic plants in Venice Lagoon, Italy and Rustico Bay, Canada—analyses of in situ measurements. Journal of Marine Systems 51: 293-308. DOI: 10.1016/j.jmarsys.2004.05.017

Wang Y, Gao S, Ke X. 2004. Observations of boundary layer parameters and suspended sediment transport over the intertidal flats of northern Jiangsu, China. Actaoceanologicasinica, 23(3), 437-448.

Wolanski E, Mazda Y, Ridd P. 1992. Mangrove Hydrodynamics. In Tropical mangrove ecosystems, Robertson AI, Alongi D (eds). American Geophysical Union: Washington D.C. 43-62.

Zhang Y, Wang W, Wu Q, Fang B, Lin P. 2006. The growth of Kandeliacandel seedlings in mangrove habitats of the Zhangjiang estuary in Fujian, China. ActaEcologicaSinica, 26: 1648-1655. DOI: 10.1016/s1872-2032(06)60028-0

Zhang Y, Huang G, Wang W, Chen L, Lin G. 2012. Interactions between mangroves and exotic Spartina in an anthropogenically disturbed estuary in southern China. Ecology, 93: 588-597

Zheng B, Liao K, Zeng Z, He J, Chen C. 2009. Study on the characteristics of tidal current dynamic in Dongshan Bay. Journal of Oceanography in Taiwan Strait, 28: 546-552

Zong L, and Nepf H. 2010. Flow and deposition in and around a finite patch ofvegetation. Geomorphology, 116:363-372. doi:10.1016/j.geomorph.2009.11.020.

Table 1. Vegetation measurements of mangrove trees and saltmarsh grasses.

Spartina	Height (m)	Coverage (%)	Biomass (dry, kg m^{-2})	Diameter (m)
	1.0	90%	2.5	0.005
Mangrove	Height (m)	Canopy closure (%)	Canopy distance* (m)	Trunk diameter (m)
	1.6	80%	0.4	0.1

*Canopy distance measures the distance from the canopy bottom to the bed

Table 2. Inter-comparison of key parameters for mudflat, mangrove edge and saltmarsh edge.

Classification	Parameter	Mean Value		
		Flat (Location A)	Mangrove (Location B)	Saltmarsh (Location C)
Flow Magnitude ($m\ s^{-1}$)	Flow speed	0.10	0.05	0.06
	U component	0.10	0.03	0.05
	V component	0.01	0.03	0.01
Flow Direction (°)	Flood flow	305	257	290
	Ebb flow	124	94	120
Energy	TKE density ($J\ m^{-3}$)	0.84	0.07	0.12
	Dissipation percentage	-	92%	86%
Bulk Property	Drag coefficient	0.04	0.35	0.16
	Tidal wave speed* ($m\ s^{-1}$)	2.2	0.8	1.8

*Note: the tidal wave speed refers to the tidal wave propagation speed within various medium and it is an indicator for refraction.

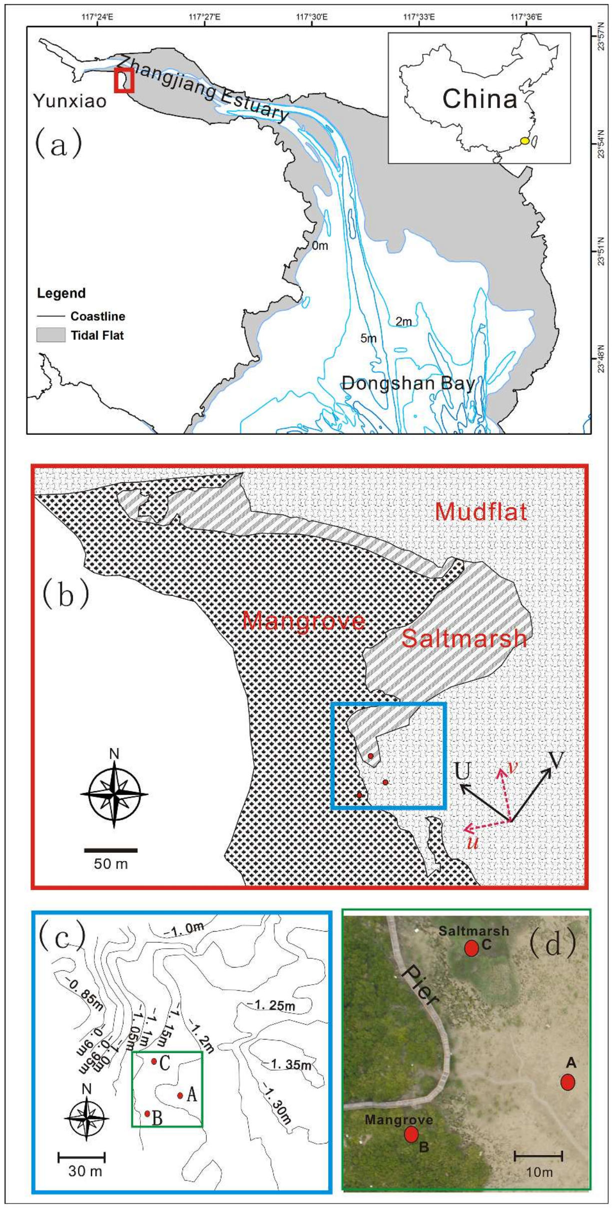

Figure 1. Location map of Yunxiao National Nature Reserve.(a)the region map of Zhangjiang Estuary. (b)vegetation distribution map and the locations of the ADV deployments; U and V indicate main flood direction and perpendicular flow components on the mudflat; u and v are the flow components perpendicular and parallel to vegetation boundaries after axis rotation. (c)topographic map of the studied area; elevation data (in meters) refers to a local benchmark of 0 m; the blank area on the upper tidal flat was covered by high mangrove trees with high canopy closure which blocked GPS signals. (d)aerial photography of the study site, showing the three measurement locations: A-bare tidal flat, B- mangrove boundary, and C- saltmarsh boundary.
284x560mm (300 x 300 DPI)

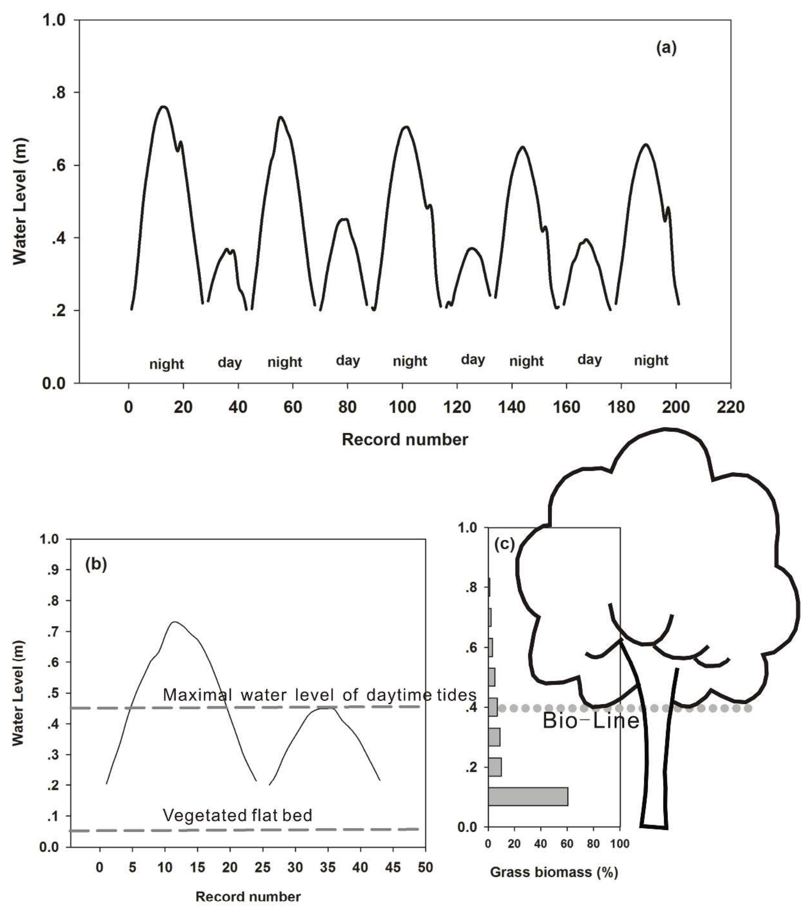

Figure 2. Water level variation and vegetation canopy characteristics: (a) water level variation throughout the measurement period (9 tidal cycles); (b) Diurnal inequality during a typical spring tide day (1st May); and (c) vertical distribution of saltmarsh canopy biomass and the bottom position of mangrove canopy which is marked as 'bio-line'. All of the elevation data are above the bed level of Location A (mud flat).
296x419mm (300 x 300 DPI)

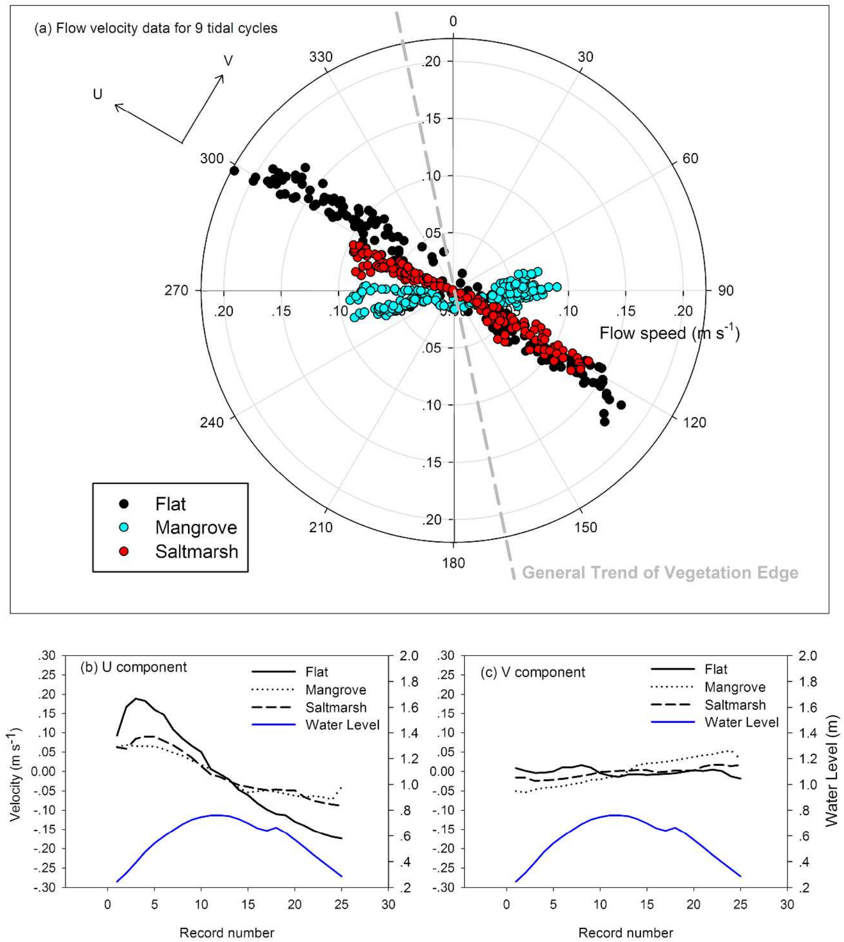

Figure 3. Flow velocity over 9 tidal cycles: (a) 5-minute averaged horizontal flow velocity data plotted in geographical direction, together with general trend of vegetation boundary position; (b) U (flood, mudflat) component variation over a spring tidal cycle; and (c) V component (perpendicular to flood) variation over a spring tidal cycle.
296x420mm (300 x 300 DPI)

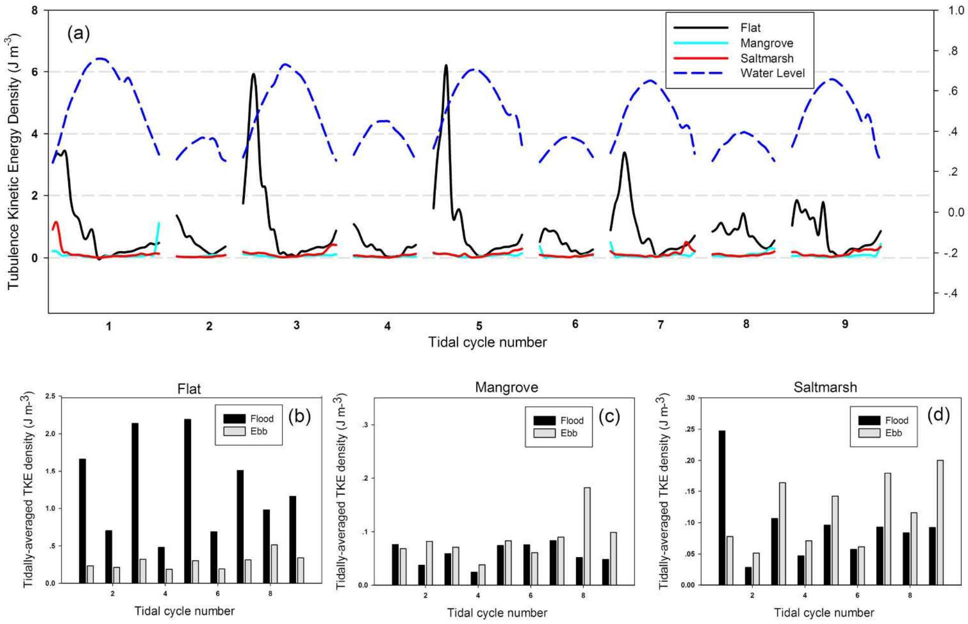

Figure 4. Turbulent Kinetic Energy (TKE) density of the three locations.(a)5-minute averaged TKE density over 9 tidal cycles, together with water level variations. (b-d) tidal cycle asymmetries of the bare mud flat (b), the mangrove (c) and the saltmarsh (d).
209x148mm (300 x 300 DPI)

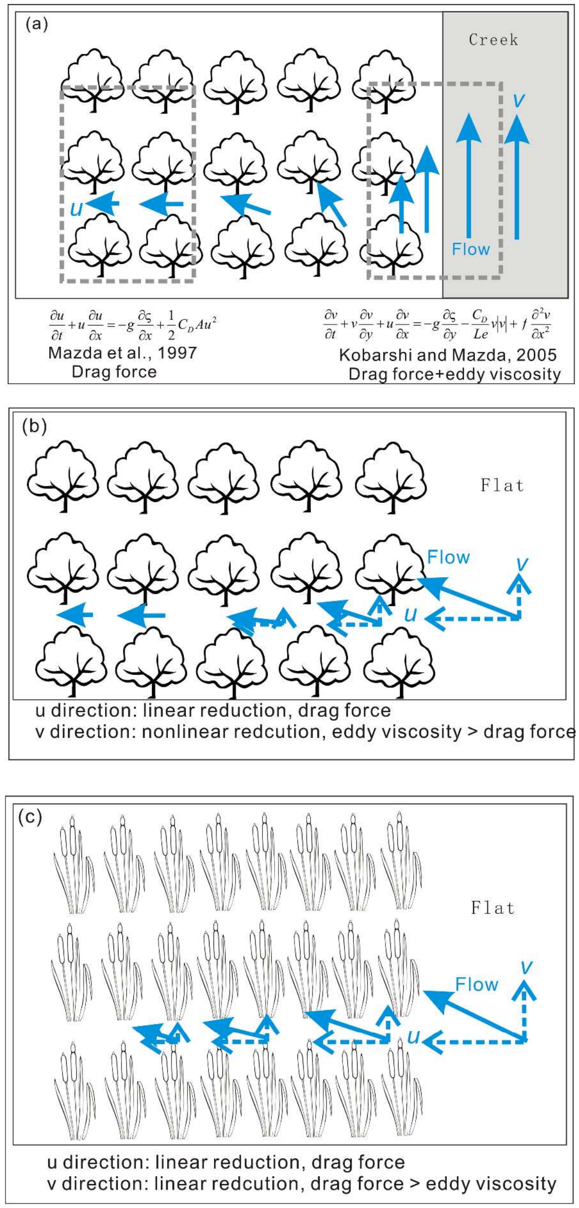

Figure 5. Schematic graph of flow variation over vegetation boundary and the associated mechanisms: (a) mechanical explanation and model equations given by previous researchers (revised based on Mazda et al. (1997) and Kobashi and Mazda (2005)); (b) flow variation over mangrove boundary and the mechanism; and (c) flow variation over saltmarsh boundary and the mechanism.
275x580mm (300 x 300 DPI)

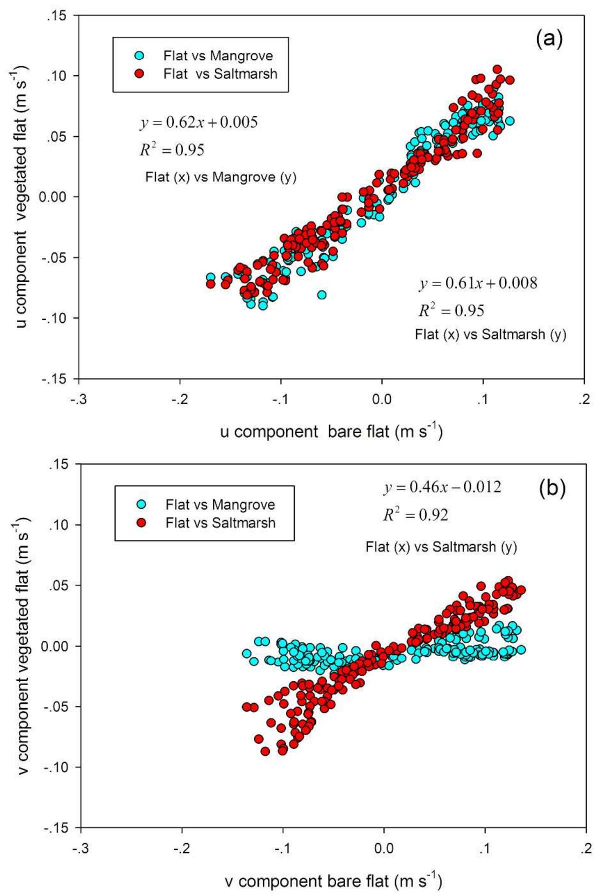

Figure 6. Relationship between flow components in mud flat, mangrove boundary and saltmarsh boundary: (a) flow component normal to the boundaries; and (b) flow component parallel to the boundaries.
296x420mm (300 x 300 DPI)

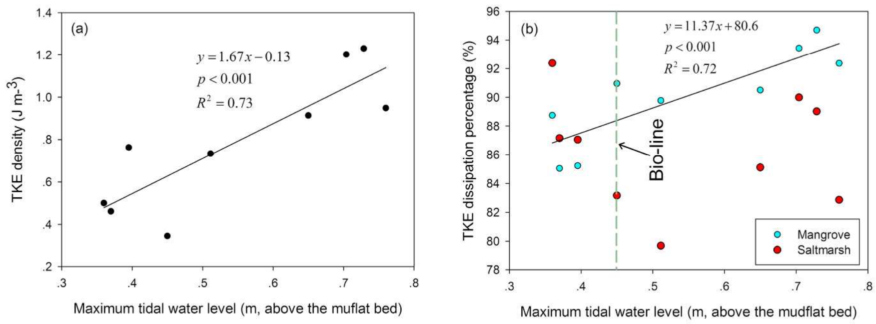

Figure 7: Turbulent Kinetic Energy (TKE) density dissipation by vegetation: (a) tidally-averaged TKE density against maximum water level of each tidal cycle; and (b) the comparison of energy dissipation percentages for two types of vegetation, in association with tidally maximum water level.
209x148mm (300 x 300 DPI)

Table 1. Vegetation measurements of mangrove trees and saltmarsh grass.

Spartina	Height (m)	Coverage (%)	Biomass (dry, kg m^{-2})	Diameter (m)
	1.0	90%	2.5	0.005
Mangrove	Height (m)	Canopy closure (%)	Canopy distance* (m)	Trunk diameter (m)
	1.6	80%	0.4	0.1

*Canopy distance measures the distance from the canopy bottom to the bed

Table 2. Inter-comparison of key parameters for mudflat, mangrove edge and saltmarsh edge.

Classification	Parameter	Mean Value		
		Flat (Location A)	Mangrove (Location B)	Saltmarsh (Location C)
Flow Magnitude ($m\ s^{-1}$)	Flow speed	0.10	0.05	0.06
	U component	0.10	0.03	0.05
	V component	0.01	0.03	0.01
Flow Direction (°)	Flood flow	305	257	290
	Ebb flow	124	94	120
Energy	TKE density ($J\ m^{-3}$)	0.84	0.07	0.12
	Dissipation percentage	-	92%	86%
Bulk Property	Drag coefficient	0.04	0.35	0.16
	Tidal wave speed* ($m\ s^{-1}$)	2.2	0.8	1.8

*Note: the tidal wave speed refers to the tidal wave propagation speed within various medium and it is an indicator for refraction.